Supporting Information

One-step synthesis of SnCo nanoconfined in hierarchical carbon nanostructures for lithium ion battery anode

Jian Qin [†, a], Dongye Liu [†, a], Xiang Zhang [a], Naiqin Zhao [a, b], Chunsheng Shi [a], En-Zuo Liu [a], Fang He [a], Liying Ma [a], Jiajun Li [a], and Chunnian He [, a, b]*

[a] School of Materials Science and Engineering and Tianjin Key Laboratory of Composites and Functional Materials, Tianjin University, Tianjin, 300072, P. R. China

[b] Collaborative Innovation Center of Chemical Science and Engineering, Tianjin 300072, China

[†]These authors contributed equally.

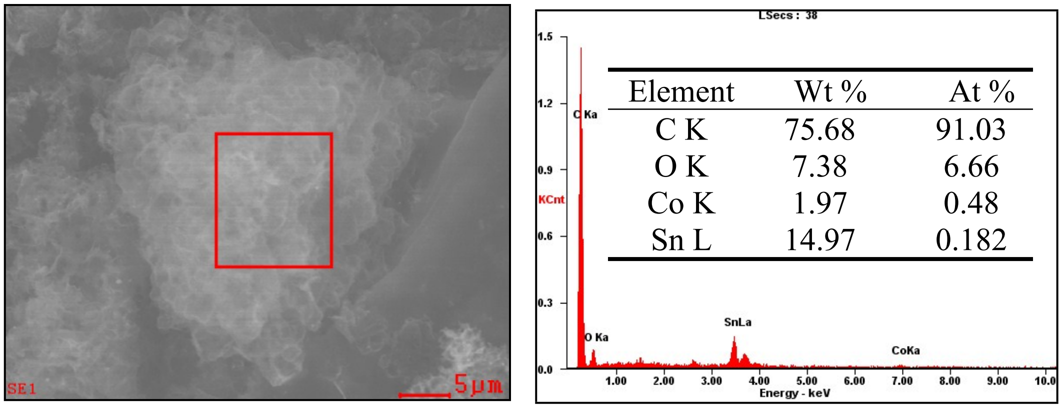

Element	Wt %	At %
C K	75.68	91.03
O K	7.38	6.66
Co K	1.97	0.48
Sn L	14.97	0.182

Fig. S1 EDS pattern of the SnCo@CNT-3DC composite.

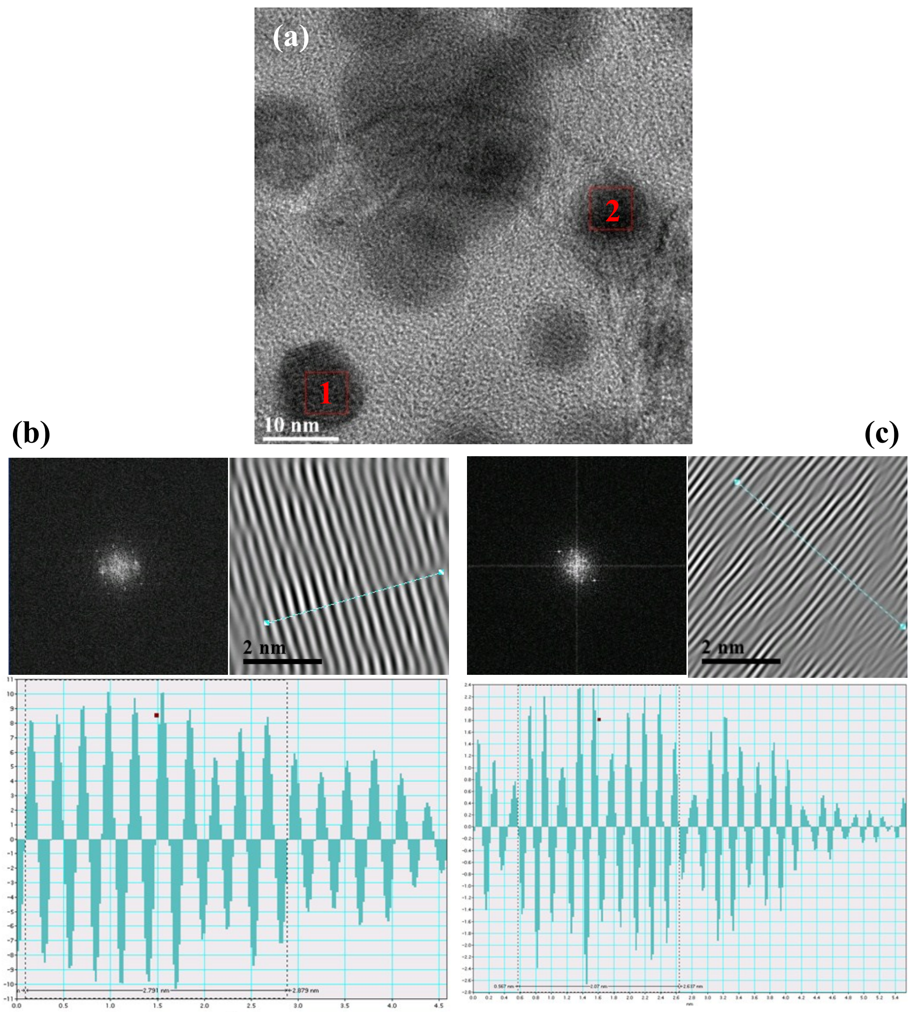

Fig. S2 (a) TEM image of the SnCo@CNT-3DC shown in Fig. 3d. (b, c) Fourier transforms and interplanar spacing measurements of particle 1 and 2 shown in Fig.S2a, respectively. The interplanar spacings of these two nanoparticles are measured to be ≈0.279 nm and ≈0.207 nm, which are well matched with the d-spacing of Sn (101) and $CoSn_2$ (202), respectively.

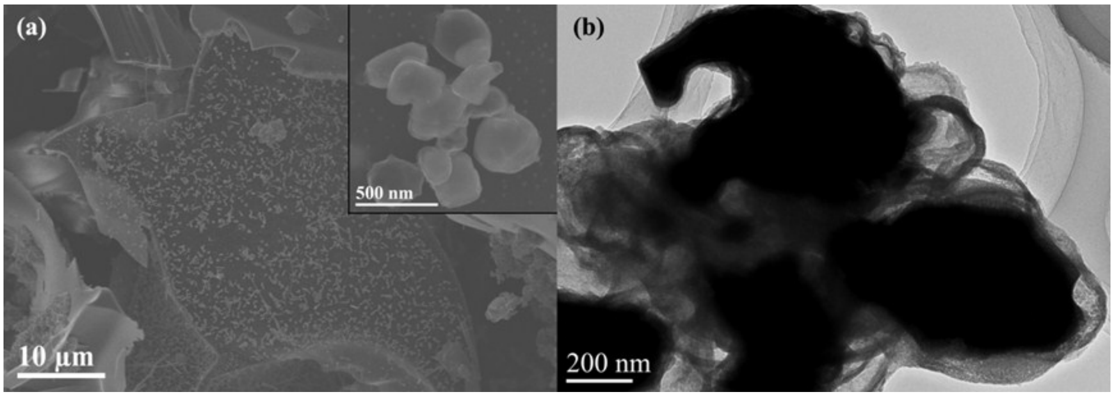

Fig. S3 (a) SEM image, (b) TEM image of the SnCo/C composite.

Table S1. Conductivity of the SnCo@CNT-3DC and SnCo/C composites.

Sample	Pressure (MPa)	Thickness (mm)	Conductivity ($S\ cm^{-1}$)
SnCo@CNT-3DC	17	0.77	109.29
SnCo/C	17	0.76	11.99

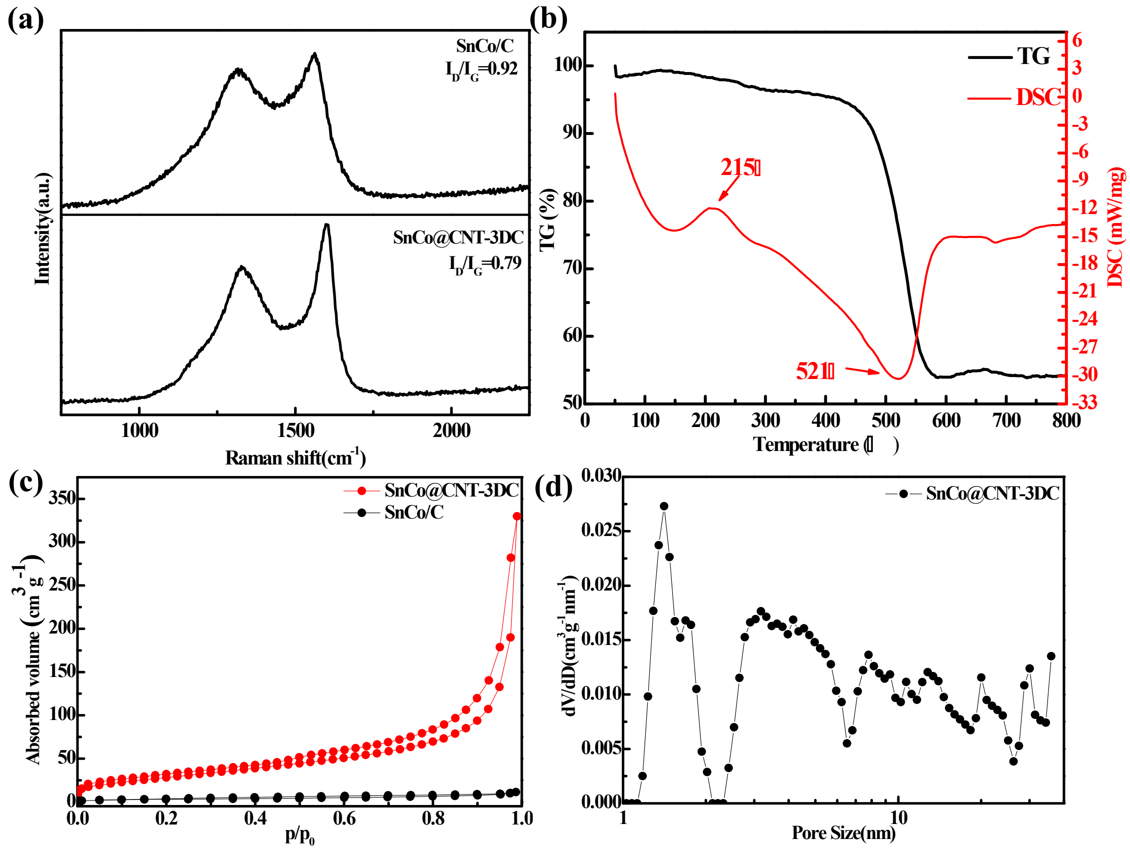

Fig. S4. (a) Raman spectrums of the SnCo@CNT-3DC and SnCo/C composites. (b) TG and DSC curves of the SnCo@CNT-3DC composite. (c) N_2 adsorption-desorption isotherms and (d) pore distribution of the SnCo@CNT-3DC composites.

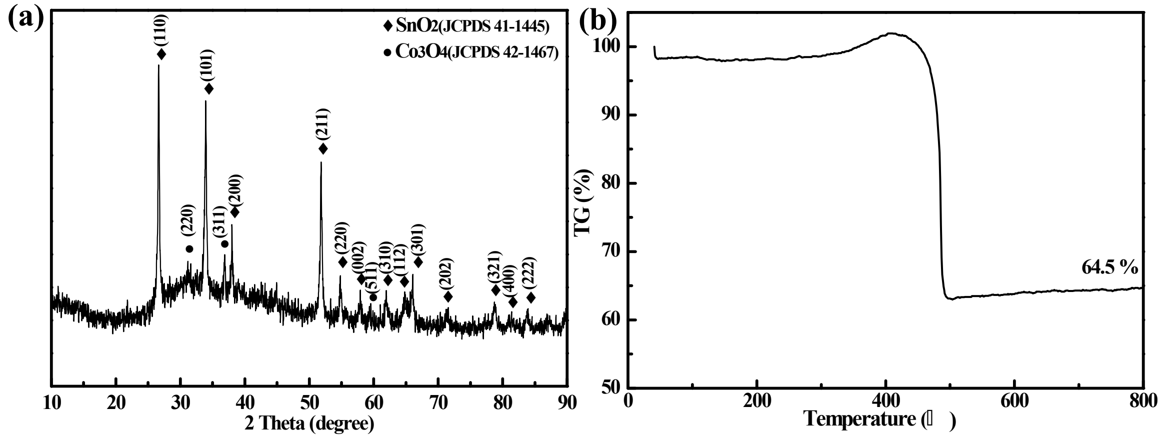

Fig. S5 (a) XRD pattern of the SnCo@CNT-3DC composite after TG test. (b) TG curve of the SnCo/C composite.

Fig. S5a shows the XRD pattern of the SnCo@CNT-3DC composite after TG test. It can be seen that the final products are SnO_2 and Co_3O_4. And the content of final products from TG analysis is 55 wt%. So, based on the atomic ratio of Sn to Co in the precursor (4:1), the Sn and Co contents are calculated using the following equation:

$$Sn\ wt\% \times \frac{SnO2(molecular\ weight)}{Sn(molecular\ weight)} + Co\ wt\% \times \frac{Co3O4(molecular\ weight)}{3 \times Co(molecular\ weight)} = 55\% \qquad \text{(S1)}$$

$$^{Sn\ wt\%}/_{Sn(molecular\ weight)} : ^{Co\ wt\%}/_{Co(molecular\ weight)} = 4:1 \qquad \text{(S2)}$$

Sn wt% = 38.2 %; Co wt% = 4.7 %

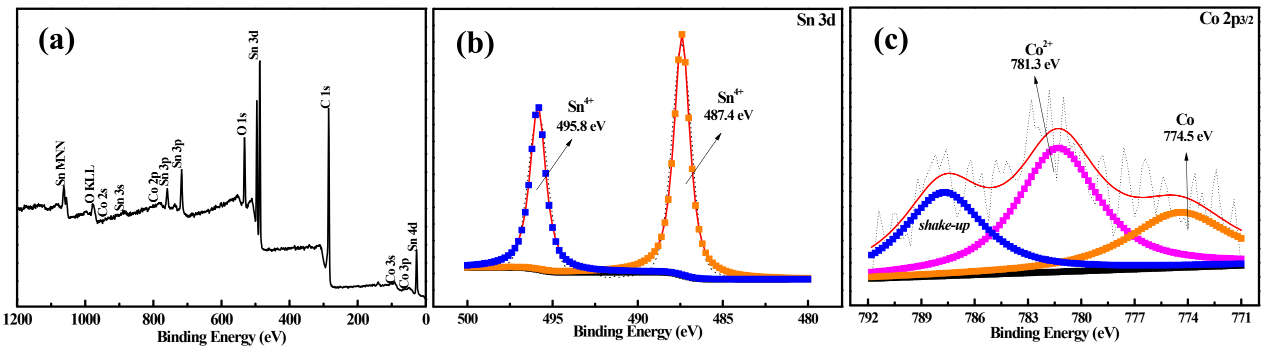

Element	C	O	Co	Sn
Content (at %)	80.94	14.15	0.38	4.53

Fig. S6 XPS spectrum of the SnCo@CNT-3DC composite.

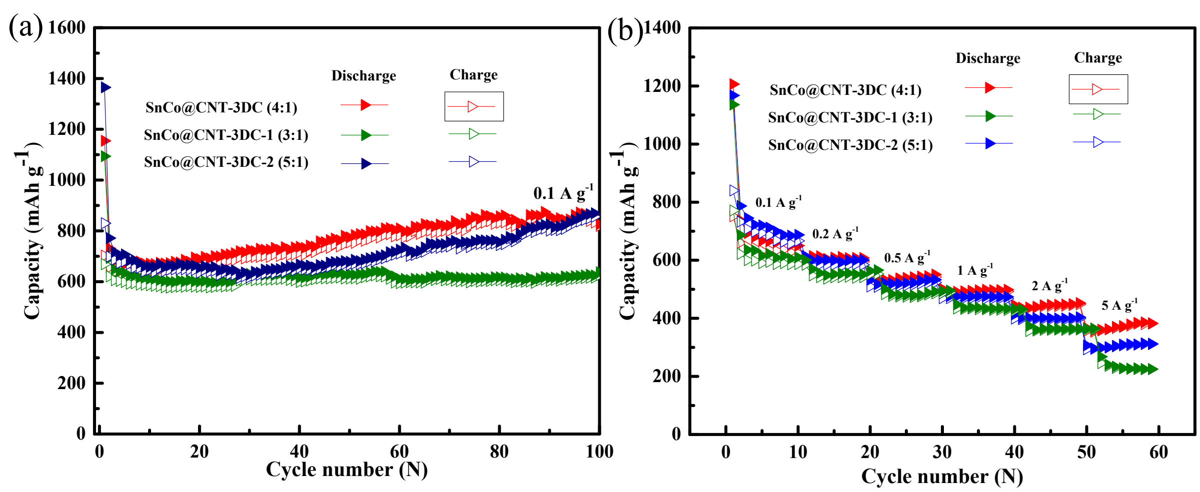

Fig. S7 (a) Cycling performance and (b) rate performance of the SnCo@CNT-3DC composites with different Sn and Co ratios, in which the SnCo@CNT-3DC (4:1) exhibits the best electrochemical performance.

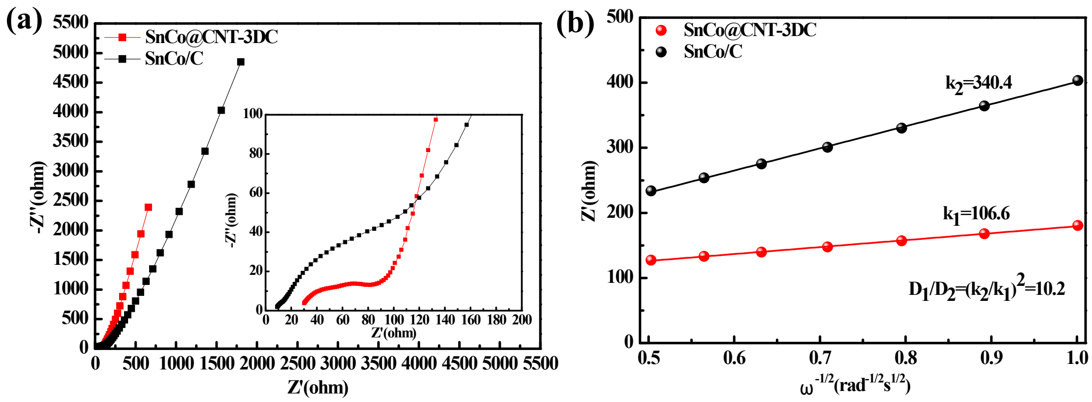

Fig. S8 (a) EIS curves of the SnCo@CNT-3DC and SnCo/C composite electrodes. (b) Calculation of Li^+ transfer coefficient of the SnCo@CNT-3DC and SnCo/C composite electrodes.

We also calculated the Li^+ transfer coefficient using equations as following:

$$D = R^2T^2/2n^4F^4\sigma 2\ wA^2C^2 \qquad \text{(S3)}$$

$$Z' = R + \sigma_w\omega^{-1/2} \qquad \text{(S4)}$$

The R, T, n, F, σ_w, A and C in equations present the gas constant, the absolute temperature, charge-transfer number, the Faraday constant, the Warburg coefficient, the electrodes' surface area and the Li^+ concentration in the electrode, respectively. Since the values of R, T, n, F, A and C in above equations are almost the same for the SnCo@CNT-3DC and SnCo/C electrodes, the diffusion coefficient of these two electrodes are in direct proportion to the square of σ_w, which is the slope of the impedance to $\omega^{-1/2}$. As shown in Figure S4b, the diffusion coefficient of the SnCo@CNT-3DC electrode is more than 10 times higher than that of the SnCo/C electrode, which is in good consistency with the result shown in Figure 6c.

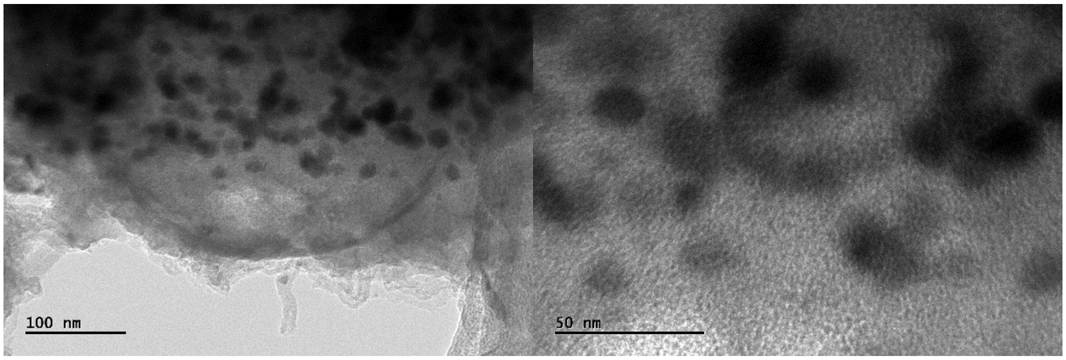

Fig. S9 (a, b) TEM images of the SnCo@CNT-3DC electrode after 100 cycles at a current density of 0.1 A g^{-1}

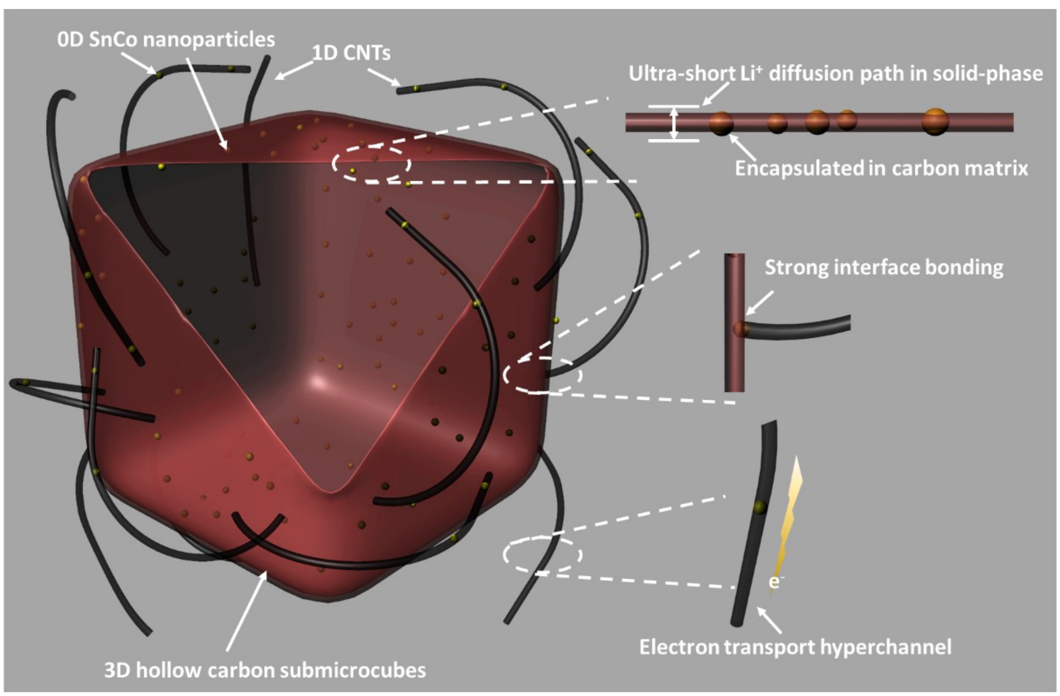

Fig. S10 Schematic illustration of structural advantages of the SnCo@CNT-3DC for lithium storage.

Table S2 Electrochemical performances of various SnCo anode materials for LIBs.

Materials	Current density ($A\ g^{-1}$)	Discharge capacity ($mAh\ g^{-1}$)	Capacity after (x) cycles	Capacity at high current density ($mAh\ g^{-1}$)
SnCo@CNT-3DC (This work)	**0.1**	**739**	**826(100)**	**450(2 $A\ g^{-1}$)**
	5	**350**	**280(1000)**	**380(5 $A\ g^{-1}$)**
Sn-Co@C [S1]	0.1	945	818(100)	472 (2 $A\ g^{-1}$)
SnCo/PAN-CNFs [S2]	0.6	560	548(100)	~280 (3.025 $A\ g^{-1}$) ~200 (6.05 $A\ g^{-1}$)
meso-$Co_{0.3}Sn_{0.7}$ [S3]	~0.7	~663	~530(50)	~400 (2 $A\ g^{-1}$)
Sn-Co@graphene [S4]	0.5	672	560(60)	~483 (0.8 $A\ g^{-1}$)
GNS-SnCo [S5]	~0.072	1100	600(60)	~500(0.72 $A\ g^{-1}$)
Sn-Co alloy film[S6]	0.148	~850	~650(60)	/
$CoSn_5$[S7]	0.1	~500	480(100)	/
$CoSn_3$-MWCNTs[S8]	0.1	~480	~350(20)	/
Co-Sn/CNF[S9]	0.161	~710	560(80)	~400(4.3 $A\ g^{-1}$)

Reference

S1 X. Shi, H. H. Song, A. Li, X. H. Chen, J. S. Zhou and Z. K. Ma, *J. Mater. Chem. A*, 2017, **5**, 5873–5879

S2 J. W. Shin, W. H. Ryu, K. S. Park and I. D. Kim, ACS Nano, 2013, **7**, 7330-7341.

S3 G. O. Park, J. Yoon, J. K. Shon, Y. S. Choi, J. G. Won, S. B. Park, K. H. Kim, H. S. Kim, W. S. Yoon and J. M. Kim, *Adv. Funct. Mater*., 2016, **26**, 2800–2808

S4 J. S. Zhu, D. L. Wang, T. F. Liu and C. F. Guo, *Electrochim. Acta*, 2014, **125**, 347-353.

S5 P. Chen, L. Guo and Y. Wang, *J. Power Sources*, 2013, **222**, 26-532.

S6 C. Yang, D. W. Zhang, Y. B. Zhao, Y. H. Lu, L. Wang and J. B. Goodenough, *J. Power Sources*, 2011, **196**, 10673-10678.

S7 F. X. Xin, X. L. Wang, J. M. Bai, W. Wen, H. J. Tian, C. S. Wang and W. Q. Han, *J. Mater. Chem. A*, 2015, **3**, 7170-7178.

S8 C. X. Zhai, N. Du, H. Zhang, J. X. Yu, P. Wu, C. M. Xiao and D. R. Yang, *Nanoscale*, 2011, **3**, 1798-1801.

S9 B. O. Jang, S. H. Park and W. J. Lee, *J. Alloy. Compd.*, 2013, **574**, 325-330.